JGR Oceans

RESEARCH ARTICLE

10.1029/2024JC021643

Marine eDNA Production and Loss Mechanisms

Elizabeth Brasseale[1], Nicolaus Adams[2], Elizabeth Andruszkiewicz Allan[1], Eiren K. Jacobson[3], Ryan P. Kelly[1], Owen R. Liu[1,2], Stephanie Moore[2], Megan Shaffer[1,2], Jilian Xiong[4], and Kim Parsons[2]

[1]School of Marine and Environmental Affairs, University of Washington, Seattle, WA, USA, [2]Conservation Biology Division, Northwest Fisheries Science Center, National Marine Fisheries Service, National Oceanic and Atmospheric Administration, Seattle, WA, USA, [3]School of Mathematics and Statistics, University of St Andrews, St Andrews, Scotland, [4]School of Oceanography, University of Washington, Seattle, WA, USA

Key Points:

- Atlantic bottlenose dolphin eDNA was sampled at near-hourly frequency, and concentrations varying by over three orders of magnitude
- A model of background eDNA production with episodic larger eDNA production events best explained near-hourly variability
- Little genetic material persisted hour to hour, and most eDNA loss was attributable to physical rather than biological processes

Supporting Information:

Supporting Information may be found in the online version of this article.

Correspondence to:

E. Brasseale,
eabrasse@uw.edu

Citation:

Brasseale, E., Adams, N., Allan, E. A., Jacobson, E. K., Kelly, R. P., Liu, O. R., et al. (2025). Marine eDNA production and loss mechanisms. *Journal of Geophysical Research: Oceans*, *130*, e2024JC021643. https://doi.org/10.1029/2024JC021643

Received 25 JUL 2024
Accepted 10 APR 2025

Author Contributions:

Conceptualization: Elizabeth Brasseale, Elizabeth Andruszkiewicz Allan, Ryan P. Kelly, Megan Shaffer, Jilian Xiong, Kim Parsons
Data curation: Nicolaus Adams, Elizabeth Andruszkiewicz Allan, Megan Shaffer, Kim Parsons
Formal analysis: Elizabeth Brasseale, Elizabeth Andruszkiewicz Allan, Ryan P. Kelly, Jilian Xiong
Funding acquisition: Elizabeth Andruszkiewicz Allan, Ryan P. Kelly, Kim Parsons
Investigation: Elizabeth Brasseale, Elizabeth Andruszkiewicz Allan, Ryan P. Kelly
Methodology: Elizabeth Brasseale, Nicolaus Adams, Elizabeth Andruszkiewicz Allan, Eiren K. Jacobson, Ryan P. Kelly, Stephanie Moore, Megan Shaffer, Jilian Xiong, Kim Parsons

Abstract Environmental DNA (eDNA) analysis is a technique for detecting organisms based on genetic material in environments such as air, water, or soil. Observed eDNA concentrations vary in space and time due to biological and environmental processes. Here, we investigate variability in eDNA production and loss by sampling water adjacent to a managed population of non-native cetaceans on a near-hourly timescale for 48 hr. We used diverse sampling approaches and modeling methods to describe time variability in observed eDNA concentrations and then compare the magnitude of production and loss mechanisms. We parsed production and loss in a conceptual box model and compared biological and physical loss rates using a decay experiment and a physical transport-and-diffusion tracer model. We then evaluated eDNA concentrations along a transect away from the animal enclosure in light of model parameter estimates. We conclude that eDNA production is best conceptualized using a time-varying mixed-state model, and biological losses are small relative to physical losses in the marine environment. Because physical loss is unsteady and nonlinear, tracer models are especially helpful tools to estimate it accurately.

Plain Language Summary Environmental DNA (eDNA) is the genetic material of animals, bacteria, or plants that can be found in air, soil, or water samples. Using eDNA for marine ecology is complicated, however, because animals may shed DNA at irregular rates and once shed, eDNA is moved by ocean currents and broken apart by microbes. To better understand the fate of eDNA, we sampled water repeatedly near an enclosure of non-native dolphins in Hood Canal, Washington to see how much eDNA concentrations changed hourly over 2 days. We compared models built on different explanations for dolphin eDNA variability. Observations were best explained by a model where dolphins shed DNA at steady background rate but could occasionally shed large amounts of eDNA (presumably through defecation). In that model, over half of eDNA was lost each hour. To distinguish biological and physical loss rates, we estimated degradation in the lab and ocean current transport and diffusion using an ocean model. The diffusion rate from the ocean model matched observed eDNA better than biological decay rates, which were much lower. By better understanding how eDNA is produced and where it goes in the ocean, we can better interpret our eDNA measurements to learn about marine ecosystems.

1. Introduction

Environmental DNA, or eDNA, is the genetic material from organisms found in air, soil, or water samples. Rapid advances in technology have made eDNA an attractive tool to complement traditional approaches for stock assessment (Fukaya et al., 2020), invasive species detection (Keller et al., 2022), measuring ecological response to environmental intervention efforts (Allan et al., 2023) and more. Animal species produce eDNA idiosyncratically (Allan et al., 2020) and eDNA evolves after being shed by the animal (Goldberg et al., 2016), leading to high temporal and spatial variability (Ely et al., 2021; Jensen et al., 2022). The mechanisms affecting eDNA concentration are not always clear. Production and loss are affected by a combination of biological processes (e.g., shedding rate which can depend on abundance or biomass of the target species (Allan et al., 2020; Jo & Yamanaka, 2022), aggregation (Yates et al., 2023)), molecular processes (e.g., decay of genetic material (Collins et al., 2018)), environmental processes (e.g., oceanic transport and diffusion (Fukaya et al., 2020; Kutti et al., 2020; Murakami et al., 2019), and sinking of cells (Allan et al., 2021)). A mechanistic framework for understanding the dynamics of eDNA in the field requires, at minimum, terms for production, loss, and process variability. Here, we build a conceptual box model by assuming our stationary samples over time are

Project administration: Elizabeth Andruszkiewicz Allan, Ryan P. Kelly, Kim Parsons
Resources: Nicolaus Adams, Elizabeth Andruszkiewicz Allan, Ryan P. Kelly, Stephanie Moore, Megan Shaffer, Jilian Xiong, Kim Parsons
Software: Elizabeth Brasseale, Eiren K. Jacobson, Ryan P. Kelly, Owen R. Liu, Jilian Xiong
Supervision: Elizabeth Andruszkiewicz Allan, Ryan P. Kelly, Kim Parsons
Validation: Elizabeth Brasseale, Elizabeth Andruszkiewicz Allan, Eiren K. Jacobson, Ryan P. Kelly, Owen R. Liu, Jilian Xiong
Visualization: Elizabeth Brasseale
Writing – original draft: Elizabeth Brasseale, Elizabeth Andruszkiewicz Allan, Ryan P. Kelly, Megan Shaffer, Jilian Xiong
Writing – review & editing: Elizabeth Brasseale, Nicolaus Adams, Elizabeth Andruszkiewicz Allan, Eiren K. Jacobson, Ryan P. Kelly, Owen R. Liu, Stephanie Moore, Megan Shaffer, Jilian Xiong, Kim Parsons

representative of the mean eDNA concentration in the near surface environment (upper 2 m) over a horizontal scale of about 10 m. We further elaborate production and loss terms to illustrate the details of particular interest.

The only source of eDNA to the conceptual box is shedding of genetic material, hereafter "eDNA production." However, eDNA production is hard to measure and consequently, many aspects of eDNA production remain poorly understood. In particular, the degree to which production varies over time has not been well studied, because laboratory eDNA shedding experiments often use models assuming steady state eDNA concentrations (Allan et al., 2020; Jo & Yamanaka, 2022). Further, there are no eDNA production estimates for marine mammals due to the logistical difficulty of keeping large animals in tanks or pools long enough to reach steady state.

Mechanisms for eDNA loss may be biological or physical. Here, eDNA loss describes decreases in detected eDNA concentration in the conceptual box. Biologically, eDNA concentration may decrease due to molecular degradation. Over time, eDNA degrades into smaller fragments that eventually become too short to amplify reliably with molecular methods (Allan et al., 2020; Collins et al., 2018). Environmental DNA decay rates are measured empirically by isolating water that starts with detectable target species eDNA and resampling over time until the signal is no longer detectable (Allan et al., 2020). Most often, decay is modeled as a first order log-linear process with published estimates of decay rate constants ranging from approximately 0.01–0.1 hr^{-1} (Allan et al., 2020; Collins et al., 2018; Jo et al., 2019). More recently, a two-phase model of degradation has been proposed wherein coral eDNA was found to decay at an elevated rate until a breakpoint, after which the degradation rate slowed (McCartin et al., 2022). Grazing by microbial organisms is generally thought to be the dominant decay mechanism, which degrades eDNA faster at higher temperatures due to microbial community composition (Allan et al., 2020; McCartin et al., 2022).

The physical mechanisms for eDNA loss include transport and diffusion of material by ocean currents. Transport is the process by which eDNA is moved by flowing water away from the source organism, and diffusion is the process by which turbulence and differential transport disperse genetic material into a lower concentration over a larger volume. Vertical transport due to circulation and settling is likely to be slower in most cases than diffusion and lateral transport (Allan et al., 2021). Resuspension, which is important in streams (Shogren et al., 2017), is likely to be unimportant for surface sampling of deeper freshwater and marine environments, which can be hundreds or thousands of meters deep. Rates of diffusion and transport are the product of local rivers, weather, tides, and topography, which are unique to each study region and not generalizable. In streams or marine systems with relatively constant mean flow rate, the effects of transport and diffusion of genetic material from a source population can be simplified into a one dimensional, steady state analytical model with varying success (Cerco et al., 2018; Lutscher et al., 2005; Shea et al., 2022; Shogren et al., 2017, 2019). In the next level of complexity, numerical model systems exist to simulate eDNA transport and diffusion through unsteady and branching riverine systems (Augustine et al., 2024; Carraro et al., 2020). However, more complexity is needed to model marine environments, which have currents that are neither unidirectional nor reasonably approximated as one-dimensional, such as tidally dominated fjords (Baetscher et al., 2024; Kutti et al., 2020) or bays (Fukaya et al., 2020; Murakami et al., 2019). To handle the complexity of these environments, primitive equation hydrodynamic models have been used to model eDNA transport and diffusion in time-varying three-dimensional current environments coupled to tracer models (Fukaya et al., 2020; Kutti et al., 2020; Xiong et al., 2025; Yamamoto et al., 2016). Multiple studies have noted that eDNA loss observed in the field is many times faster than lab-measured degradation, indicating that environmental transport and diffusion are likely to be the dominant loss mechanisms in many real-world environments (Ely et al., 2021; Murakami et al., 2019; Shogren et al., 2019). However, a quantitative assessment of eDNA production and loss mechanisms in the field is lacking.

Here, we aim to address this gap in our understanding of eDNA production and loss by (a) distinguishing production variability from loss variability in an eDNA time series and (b) differentiating losses from biological degradation versus oceanic transport and diffusion. To do so, we sampled in a nearshore environment surrounding a population of Atlantic bottlenose dolphins (*Tursiops truncatus*) housed along the eastern bank of Hood Canal in Washington state, USA. Because this is a non-native species in the Pacific Ocean, any Atlantic bottlenose dolphin eDNA found in Hood Canal can be traced back to this population. We found that a model with variable production rates best explained eDNA abundance, and that the loss rates estimated by the conceptual box model were best explained by physical processes. Although we were motivated by monitoring marine mammals at a particular site, the methodology and concepts are generalizable to eDNA time series with known point sources.

2. Data and Methods

This study incorporated diverse data sources and analysis tools to investigate variability in eDNA production rates and compare eDNA loss rates from different mechanisms. For clarity, we break both methods and results into two parts. Part 1 estimated variability in production and net loss using data from near-hourly eDNA field sampling at a single location near captive dolphins analyzed in a box model that used reported number of dolphins in the sampled pen as a predictor of observed eDNA concentrations. Part 2 quantified competing loss mechanisms using a lab-based eDNA degradation experiment, a field-based transect sample, and a computer tracer model of eDNA transport and diffusion.

Note that different protocols were used to sample, process, and quantify eDNA for the different parts of the study (detailed below). In Part 1, we used an autonomous environmental sampler and followed the protocol recommended by the manufacturer. In Part 2, samples were filtered with handheld vacuum pumps and preserved based on what was most practical for the laboratory-based decay experiment (Longmire's lysis buffer) and the field-based transect samples (self-preserving filters). We used extraction protocols that were most appropriate for each preservative. Logistically, only the samples in Part 1 could be quantified with droplet digital PCR (ddPCR). The samples in Part 2 were quantified via quantitative PCR (qPCR) but importantly both parts used the same molecular assay. We did not directly compare samples processed with different preservation treatments. Rather, we compared the relative rates of change as a function of time or location of sampling derived from sets of samples that were treated in the same way.

2.1. Description of Study Area

Hood Canal is the naturally occurring western arm of the glacially carved Puget Sound estuary, a branch of the Salish Sea on the west coast near the U.S./Canada border. Near the study site, Hood Canal is about 2.5 km wide and more than 100 m deep at its deepest point. Semidiurnal tides provide the strongest currents up to 50 cm s^{-1}. Inputs from many small rivers create a buoyant layer in the upper 10 m with subtidal seaward flow. A shallow (<50 m) sill at the mouth of Hood Canal can retain deep water for months between intermittent flushing events from intrusions of oceanic water at depth (Mofjeld & Larsen, 1984).

A small managed population of non-native Atlantic bottlenose dolphins (*Tursiops truncatus*) resides along the eastern bank of Hood Canal, WA. During winter (our study period), the dolphins spend most of their time within a closed pool with warmed water. The dolphins periodically occupy a 10 × 10 m netted enclosure open to Hood Canal for husbandry activities (Figure 1). Both the closed pool and netted enclosure are adjacent to a large concrete pier on the shallow eastern bank of Hood Canal in 10 m deep water (Figure 1b). Most of the pier is constructed on pilings through which water can flow freely except for one solid section, which blocks flow (Figure 1b). The netted enclosure allows for exchange between the enclosure and the ambient marine environment, but it is attached to the shoreward side of the solid portion of the pier and insulated from open channel currents.

2.2. Part 1: Variability in eDNA Production and Loss Using High Frequency Time Series of Dolphin eDNA

To investigate variations in production and loss, samples were collected using an autonomous sampler adjacent to the netted enclosure on a near-hourly schedule over a 48 hr period and compared the observed concentration of bottlenose dolphin eDNA with the number of dolphins occupying the netted enclosure.

2.2.1. Continuous Autonomous Water Sample Collection

We used an Environmental Sample Processor (ESP, Scholin et al. (2018); Sepulveda et al. (2020)) to autonomously collect water samples from a fixed location between the netted enclosure and the solid pier (separated by 1 m). The ESP was deployed inside a waterproof housing on the solid pier to facilitate access to wired power (Figure 1a). An external sampling subsystem designed by the Monterey Bay Aquarium Research Institute (MBARI) consisting of a submersible pump (P-10150, 12 V Mini-Typhoon Plastic Pump, Proactive Environmental Products) connected to a phase separator/pressure sampling module with tygon tubing (Yamahara et al., 2015) was used to bring water to the ESP. The sampling port of the ESP itself was positioned inside the chamber of the phase separator/pressure sampling module. The intake of the pump was placed inside a piece of open-ended perforated 3" diameter PVC pipe that was affixed to a floating dock at ∼0.5 depth. The pump

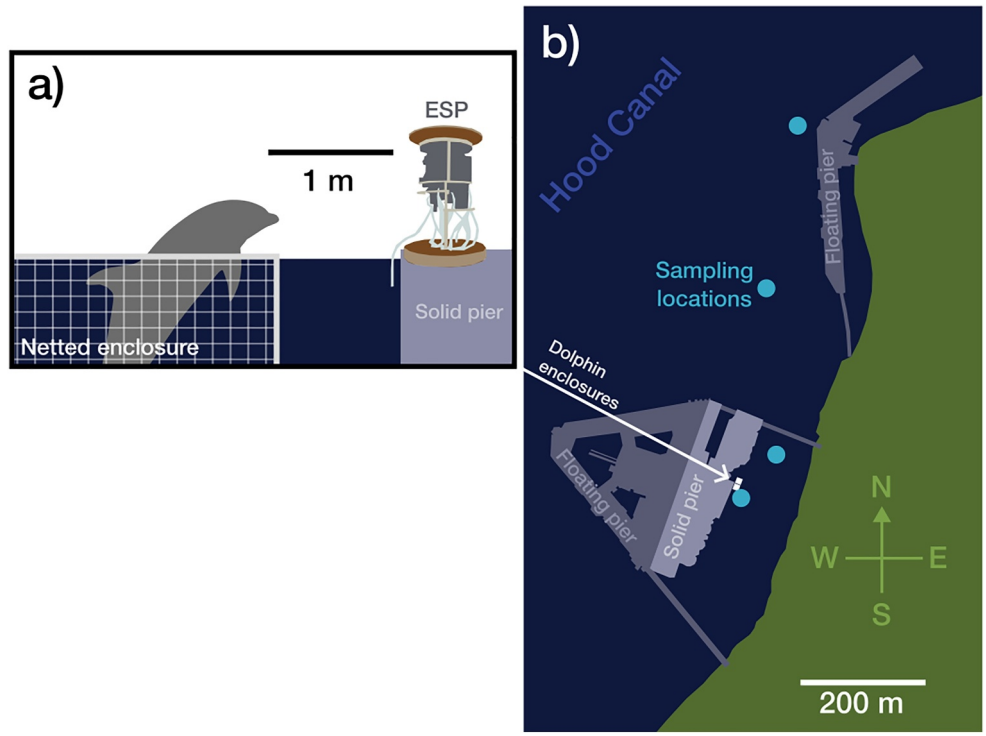

Figure 1. (a) Environmental Sample Processor (ESP) deployment relative to a netted enclosure often occupied by dolphins for husbandry activities. (b) Dolphin enclosure locations (two white squares; north is netted enclosure and south is heated pool) and transect sampling station locations (blue circles) relative to shoreline and piers.

automatically turned on and flushed the tygon tubing for 3 min prior to each sampling event. In between every sample, the ESP cleaned the sampling port with 0.2% sodium hypochlorite solution. A more rigorous cleaning with a 20% bleach solution was conducted every fifth sample.

A predeployment quality control sample was collected. This quality control sample is essentially a filter blank where the ESP filtered 2 L of Nanopure^{TM} water and applied a preservative to the filter using the same process that was used in the field. The filter blank was used to check for any contamination that was present in the ESP fluidics system at the beginning of the deployment and was analyzed along with samples that were collected in the field. At the deployment location, the ESP autonomously and continuously filtered and preserved water samples over the course of 48 hr. The target sample volume was 2,000 mL collected on 25 mm mixed cellulose ester (MCE) filter membranes with 5 μm pore size. Once the target volume was filtered, which took an average of 37 min (standard deviation 24 s), the excess water was cleared from the filter and two applications of 2 mL of RNAlater preservative was added to the puck, soaking the filter for 2 min each time. At the end of each application, the excess preservative was cleared and the sample was stored onboard the ESP. The ESP was programed to begin collecting the next sample 10 min after completing the collection and preservation of the prior sample as well as the cleaning routine. On average, the mean time between the start of filtration for consecutive samples was 70 min (standard deviation of 3 min). Because the ESP can only process one sample at a time, each sample consists of a single biological replicate.

Sampling began on 31 January 2023 at 00:50:18 UTC and 42 samples were collected over the 48-hr instrument deployment. Pump failure resulted in a reduced volume (1,875 mL) for the final sample, which ended on 2 February 2023 at 01:51:06 UTC. Preserved filters were stored onboard the ESP inside the waterproof housing at ambient temperature (~4–16°C) and humidity (~50–70%) levels until the ESP was returned to the laboratory on 3 February 2023. The ESP was removed from its housing on 6 February 2023 and all filters were aseptically recovered into 2.0 mL screw cap centrifuge tubes and stored at ~− 80°C. DNA extraction occurred within 1 week of sample collection.

2.2.2. Quantification of Dolphin eDNA

We extracted eDNA from the filter membranes using a modified protocol of the Qiagen Blood and Tissue Kit following Walz et al. (2019). Extracted DNA was evaluated for the presence of chemical or environmental PCR inhibitors by spiking an internal positive control (IPC) into the qPCR template and comparing the cycle threshold (Ct) value of the IPC in each environmental sample compared to the Ct value of the IPC in a no template control (NTC) within a qPCR assay. A Ct shift greater than two standard deviations from the mean of the NTC + IPC controls was determined to be indicative of the presence of PCR inhibitors. None of the samples were inhibited by this metric. Extracts were then quantified with ddPCR using the regionally species-specific assay designed to detect the target species, Atlantic bottlenose dolphin (*Tursiops truncatus*). The assay was deemed regionally species-specific during testing and development because it was found to amplify a few off-target dolphins and cetaceans that are closely related to *T. Tursiops* but are not found in Puget Sound. The results of sensitivity and specificity testing and thermocycling parameters can be found by Xiong et al. (2025), and the final primer and probe sequences are in Supporting Information S1. The QX200 Droplet Digital PCR System (Bio-Rad) was used to generate droplets, amplify eDNA, and read droplets. All samples were run with $\sim$40,000 droplets per sample across two plates that each included both positive and negative controls. See the Supplemental Information for amplification conditions and post-processing of ddPCR data. Units for reported values are copies of eDNA per mL of filtered seawater.

2.2.3. Dolphin Abundance

Individual dolphins were moved into and out of the pen for husbandry activities during the experiment so that the number of dolphins occupying the netted enclosure varied over time. The number of dolphins occupying the enclosure was reported as a whole number (from 0 to 3) at a single timepoint hourly. This reporting does not reflect variations in occupancy during the hour. To match up with the ESP sampling schedule, the dolphin occupancy report was processed into minute increments such that dolphin occupancy was constant for 60 one-minute intervals then changed as a step function to the next value. The relevant reported dolphin occupancy, N_t, was calculated as the mean reported dolphin occupancy during the 37 min of active filtering associated with each eDNA sample with observed eDNA concentration y_t.

2.2.4. Conceptual Box Model

Production and loss were characterized by fitting a hierarchical Bayesian state-space model to the eDNA time series observed near the netted enclosure. Hierarchical models layer an underlying process model within an observation model to account for expected observation stochasticity in the data. The laboratory ddPCR concentration estimates were used in the Bayesian model as the observed eDNA concentration, y_t. Observations were expected to be log-normally distributed around the mean true concentration of eDNA in the water, μ_t, with variance, σ^2,

$$y_t \sim Lognormal(\mu_t, \sigma^2) \tag{1}$$

Note the σ^2 of the log-normal distribution is related to the coefficient of variance of the normal distribution, θ, by $\sigma^2 = \log(1 + \theta^2)$.

The process model determining the expected eD NA concentration at time t, μ_t, was specified as a function of the fraction of persisting eDNA from the previous sample, μ_{t-1}, plus newly produced eDNA, which were not lost to biological or physical loss mechanisms. We tested different mathematical models for Loss and Production (Table 1), but all process models had the same conceptual form (written in a finite difference approximation to highlight the sampling period length):

$$\mu_t = (1 - \Delta t \text{Loss}_{t-1})\mu_{t-1} + \Delta t \text{Production}_{t-1} \tag{2}$$

where Δt is the length of time between data points. The units of μ_t and μ_{t-1} are DNA copies mL^{-1} filtered seawater. In Equation 2, Loss and Production are not variables calculated directly but conceptual placeholders for different models, which could be time-varying or constant. However, the units of the Loss and Production models are set by the conceptual model. The Loss model has units of hr^{-1}, and the Production model has units of DNA

Table 1
List of Production and Loss Process Models Used to Evaluate Time Variation in High Frequency Dolphin eDNA Time Series, the Median Fitted Values of Model Parameters (μ_{init}, and the First Model Data Point

Model name	$1 - \Delta t$ loss	Δt production	μ_{init}	θ	α	β	ψ	ϕ	p	γ	WAIC
M1 Constant Production and Loss	α	β	46.1	6.4	0.00836	1,170	-	-	-	-	358
M2 Linear dolphin	α	$N_t\beta$	5.69	2.89	0.642	3.38	-	-	-	-	354
M3 Exponential dolphin	α	$\beta e^{\psi N_t}$	8.37	2.89	0.299	4.04	0.46	-	-	-	356
M4 Mixed-state dolphin	α	$N_t\beta(1 + z_t\phi)$	5.5	1.41	0.334	1.34	-	94.6	0.161	-	316
M5 Tidal loss	$\alpha + \gamma \frac{SSH_t - SSH_{t-1}}{H + SSHt}$	β	8.41	2.97	0.277	6.54	-	-	-	0.0238	356
M6 Random loss	α_t	β	7.77	2.77	0.307–0.741	5.05	-	-	-	-	354

Note. θ, the model CV; α, the eDNA persistence fraction (constant except for last two models, then it is time-varying); β, the background or constant eDNA production rate; N_t, the number of dolphins occupying the enclosure; ψ, the rate that shedding increases with additional dolphins in the exponential dolphin model; ϕ, the scale of increase during elevated shedding events; and γ, the scale of the tidal effect), and WAIC, a model selection criteria. For WAIC, lower is better. Units are in Table 2. Confidence intervals and other statistics for fitted parameters in Table S2 in Supporting Information S1. These values were calculated using a 70 min time step.

copies mL^{-1} hr^{-1}. The Loss model was fit functionally as an autoregressive model using variations on a unitless parameter, $\alpha = 1 - \Delta t$Loss. This is described in more detail below, and units are summarized in Table 2.

We compared models with various formulations for Production and Loss (Table 1), where parameters given in Table 1 substitute for the terms "Production" and "Loss" in Equation 2. Models that included variability in both Production and Loss were tested but are not shown here because they performed slightly worse than models that varied Production alone. eDNA production was modeled three ways. The first model assumed constant production of eDNA, ΔtProduction $= \beta$ (M1 Constant Production and Loss). The next model assumed that eDNA production scaled linearly with dolphin abundance $N_t\beta$ (M2 Linear dolphin). We also investigated whether eDNA production scaled exponentially with dolphin abundance, $\beta e^{\psi N_t}$, where ψ is a fitted parameter describing how much production rate accelerates with dolphin abundance (M3 Exponential dolphin). Finally, we tested a mixed-state model where a linear eDNA production rate per dolphin could change in a simple and restricted way by alternating between two values, a lower background production rate, and an episodically elevated production rate (M4 Mixed-state dolphin). The mixed-state model is presumed to capture defecation or other unobserved biological processes which could stochastically increase eDNA concentrations. Mixed-state model Production was modeled,

Table 2
Glossary of Variables

Variable	Description	Units	Type	Prior distribution
y	Observed eDNA concentration	copies mL^{-1}	External data	-
μ	Unobserved mean eDNA concentration	copies mL^{-1}	Modeled variable	-
μ_{init}	Initial value of μ	copies mL^{-1}	Fit constant	Uniform (1, 10,000)
θ	CV of log-normal observation model	(None)	Fit constant	Normal (0.025, 1) (Lower limit 0)
α	eDNA persistence fraction ($1 - \Delta t$ Loss)	$time^{-1}$	Fit constant	Uniform (0, 1)
β	eDNA production term (Δt Production)	copies mL^{-1} [M1, M3, M5, M6], copies mL^{-1} $dolphin^{-1}$ [M2, M4]	Fit constant	Uniform (1, 10,000)
ψ	Exponential model scale	$dolphin^{-1}$	Fit constant	Uniform (0.001, 10)
ϕ	Scale of β during elevated shedding state	(None)	Fit constant	Lognormal (5, 5) (Lower limit 10)
p	Scale of probability of elevated shedding state	$dolphin^{-1}$	Fit constant	$\frac{1}{mathrmmax(N)}$ Beta(5,5)
γ	Scale of tidal effect term	(None)	Fit constant	Normal (0,10)
Δt	Model time step	Time	External data	-
z	Binomial state variable (0 or 1)	(None)	Modeled variable	-

$$\Delta t\text{Production}_t = N_t\beta(1 + z_t\phi),$$
$$z_t \sim Binomial(1, pN_t). \quad (3)$$

Here, z_t was either 0 or 1, such that when $z_t = 0$ the production model is the same as M2 Linear Dolphin model, and when $z_t = 1$, the production model is increased by a fitted scale, ϕ. This indicates whether excess eDNA production (e.g., defecation) occurred during sampling period t. The probability that any sampling period would be in a high-production state was pN_t increasing linearly with N_t at a fitted scale p. The mixed-state model is a novel way of mathematically conceptualizing eDNA production, but it is consistent with previous models which used two size classes of eDNA particles (Allan et al., 2021) and observations that genetic material is intermittently aggregated (Yates et al., 2023).

We tested models of Loss as constant ($1 - \Delta t\text{Loss} = \alpha$) (Models M1-M4) as a constant plus a time-varying tidal component, $\alpha + \gamma \frac{SSH_t - SSH_{t-1}}{H + SSH_t}$ (M5 Tidal loss), or with loss allowed to vary randomly to account for stochastic loss mechanisms which are difficult to model (M6 Random loss). Since Hood Canal tides form a standing wave, sea surface height perturbation from mean lowest low water level (SSH) was used as a proxy for eDNA loss to tidal current effects (Mofjeld & Larsen, 1984). SSH ranged from 0 to 3.0 m above mean lowest low water during this time period. SSH was downloaded from the NOAA Bangor station tide gauge (Station ID 9445133, tidesandcurrents.noaa.gov). The depth of water at the dolphin pen, $H_0 = 10$ m, is added to SSH to get the full water column depth. For comparison, tidal currents in Hood Canal during our study period peaked at 0.5 ms^{-1}.

We used the R package 'NIMBLE' to fit each model and estimate the parameters of interest (de Valpine et al., 2017, 2024b, 2024a). Priors for the fitted parameters are summarized in Table 2 with explanations for priors Text S3 in Supporting Information S1. On the whole, our priors were weakly informed or flat. We used a Markov Chain Monte Carlo (MCMC) sampler with 1,000,000 iterations along four chains. We used the Gelman-Rubin diagnostic (Gelman & Rubin, 1992) to evaluate model convergence. The explanatory power of these process models was compared using Watanabe-Akaike Information Criteria (WAIC), which is a quantitative model selection tool with lower numbers indicating better model performance (Watanabe, 2013).

The box model is fit with $\Delta t = 70$ min, the time between ESP data points. To compare with results in Part 2 and previous studies which report hourly rates, we converted Production and Loss formulas using Δt. Using the constant loss model as an example, the model-derived α using the 70-min time step was converted to conceptual hourly loss rate using the formula,

$$\text{Loss} = (1 - \alpha)\frac{1}{70\text{min}}$$
$$\text{Loss} = (1 - \alpha)\frac{60\text{min}}{70\text{min}}\frac{1}{1\text{hr}} \quad (4)$$

2.3. Part 2: Estimating Contributions to eDNA Loss

Observations in the time series described above allowed us to estimate a total rate of eDNA loss but did not distinguish between loss due to biological degradation versus oceanic transport and diffusion. To estimate loss due to biological degradation in isolation, we performed an eDNA decay experiment. Then, to investigate the effects of environmental transport and diffusion, we collected samples at four locations along a transect away from the pen where eDNA would only be present after being exposed to biological degradation and advection and diffusion by currents. We modeled the effects of advection and diffusion at the transect sampling locations using a particle tracking model forced with the flow fields from a high-resolution hydrodynamic ocean model described further below.

2.3.1. eDNA Decay Experiment

The rate of biological decay of Atlantic bottlenose dolphin eDNA from the surface waters in Hood Canal in winter was estimated by removing approximately 25 L carboy of water from inside the netted enclosure at the time of the ESP deployment and subsequently analyzing subsamples of water over time. The carboy was then transported back to the University of Washington campus in Seattle, WA, 33 km away from the field study site and kept

outside subject to similar weather. The carboy was stored closed. Ambient atmospheric temperatures averaged 7° C during the decay experiment. Three 1 L replicates of water were subsampled and filtered over a 5 μm pore size MCE filter at 0, 2, 4, 6, 17.5, 24, 48, and 120 hr after water collection. Water was homogenized by shaking and stirring the carboy before subsampling and filtering. The filters were preserved in Longmire's buffer until eDNA extraction within 2 weeks of filtration. We extracted eDNA from the filters using a phenol-chloroform-isoamyl alcohol isolation following Ramón-Laca et al. (2021), and dolphin eDNA was amplified by qPCR in triplicate using the regionally species-specific *Tursiops truncatus* assay. We tested for inhibition and results indicated that all samples were uninhibited. Nine eDNA concentration estimates were produced per time point, comprising the three technical replicates of each of the three biological replicates. Decay was then modeled as a first-order log-linear function of time to calculate the decay rate constant in units of hr^{-1}.

2.3.2. eDNA Transect Sample Collection and Processing

Using a small boat, we filtered triplicate 3 L samples of water at each of four locations: <10, 100, 300, and 600 m away from the dolphin netted enclosure in a transect extending roughly north (blue circles in Figure 1b). These transect samples were taken on 3 February 2023 between 12:50 and 13:15 PDT, approximately 48 hr after the last ESP sample, collected via vacuum pump (Smith-Root Citizen Science Sampler; Smith-Root, Inc., USA) and were filtered onto a self-preserving MCE filter with 5 μm pore size. Filters were stored in the dark at room temperature for a week until eDNA was extracted using a Zymo Quick-DNA Miniprep Plus Kit, following the manufacturer's protocols but scaling up the volumes to 2 ml of the first lysis BioFluid and Cell Buffer (which fully submerged the filter). Each extract was then quantified using qPCR as described in the supplemental material. None of the transect samples were found to be inhibited. Quantified eDNA concentrations for the three biological and three technical replicates per filter were averaged to compare with the tracer model prediction, described next.

2.3.3. Ocean Model and Particle Tracking

To model the rates of ocean advection and diffusion of eDNA molecules, we compared the transect samples with a tracer model of local flow pathways. The tracer model used the velocity flow field output from a regional ocean model to simulate where particles bearing genetic material might end up if they were passively transported by ocean currents. Similar tracer models have been used to predict marine eDNA distributions by Allan et al. (2021); Fukaya et al. (2020); Kutti et al. (2020); Xiong et al. (2025). We used this tracer model first to assess whether our observed eDNA concentrations from transect sampling were consistent with modeled ocean transport and diffusion, and then to calculate transport and diffusion rates using the ages of particle tracers at the transect sampling locations.

Local circulation was simulated using a three-dimensional hydrodynamic model built using the Regional Ocean Modeling System (ROMS (Shchepetkin & McWilliams, 2005),). The grid has 10-m resolution in the area immediately around the dolphin enclosure and 20-m resolution extending across the channel (the same model used by Xiong et al. (2025), more details in Supporting Information S1). Using the output of the high-resolution ocean model, we simulated transport of Atlantic bottlenose dolphin eDNA away from the netted enclosure by marine currents using Tracker, a Lagrangian particle tracking software (Xiong & MacCready, 2024). The software advects particles from their start location using hourly snapshots of flow fields from the ROMS model output. Particles are advected using a 4th-order Runge-Kutta method with a 300-s time step. Vertical mixing was modeled using a modified random walk algorithm (Visser, 1997).

Ten thousand virtual particles were released hourly for four days (96 releases) leading up to the real-world transect sampling, at start locations evenly spaced along the sea surface within a 10 m by 10 m rectangle centered on the coordinates of the dolphin netted enclosure. We assumed neutrally buoyant particles, neglecting the effects of settling or floating of particles containing genetic material. Particles were nevertheless free to move vertically due to vertical advection and mixing. Each particle represented a possible transport path by which passive molecules bearing genetic material might travel. To compare with the eDNA concentrations observed in the transect sampling, a particle concentration was calculated by counting the particles in the upper 2 m of water within a 15-m radius of each sampling location. The results were not sensitive to radius choice as long as the radius was less than 75 m. The particle count was divided by the volume of the 2-m deep, 15-m radius cylinder centered on the sampling location.

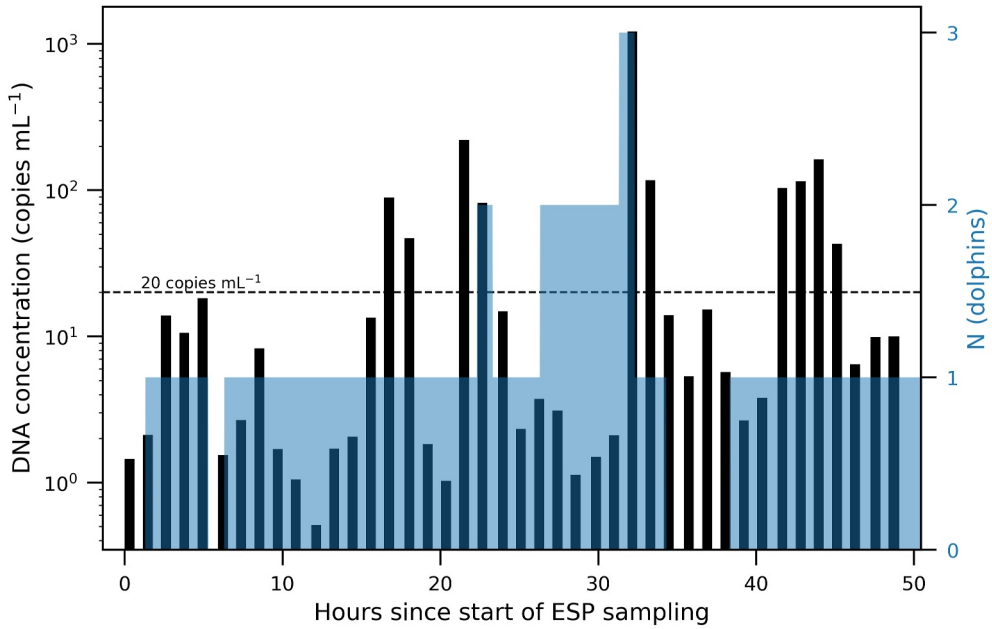

Figure 2. Black bars are dolphin eDNA concentration in water samples taken outside netted enclosure by the Environmental Sampling Processor (ESP). The ESP filtered 2,000 mL of water near-hourly for 48 hr. Gaps between black bars illustrate when the ESP was busy preserving samples and conducting cleaning routines and not actively sampling. Peaks discussed in text are samples which exceeded 20 copies mL^{-1} filtered seawater (black dashed line). Blue fill is reported dolphin occupancy as an integer value over each hour.

3. Results

3.1. Part 1: Variability in eDNA Production and Loss

3.1.1. High Frequency Dolphin eDNA Observations

Dolphin eDNA concentrations adjacent to the netted enclosure varied substantially over the 48-hr duration of sampling (Figure 2), ranging from 0.5 to 1,218 copies mL^{-1} of filtered seawater, with a mean of 56 copies mL^{-1} and a median of 6 copies mL^{-1}. Observations of eDNA concentration were non-normally distributed as illustrated by the order-of-magnitude difference between the observed mean and the median. Rather, the time series was characterized by a background eDNA concentration between 1 and 10 copies mL^{-1} punctuated by time points where concentrations peak above 20 copies mL^{-1} (indicated by dashed line Figure 2). Four distinct peaks greater than 20 copies mL^{-1} were observed beginning at hours 16, 22, 33, and 43 (Figure 2). All peaks occurred when dolphins were reported as present in the netted enclosure (bars overlapped by blue Figure 2). The average time between peaks was 10 hours. Peaks persisted for multiple time steps. The two data points with the highest eDNA concentrations were over 100 times greater than the preceding data point, then eDNA concentrations decreased by 90% steadily for the three samples following the initial peak in a sawtooth pattern (Figure 2).

3.1.2. Production and Loss Model Fitting and Comparison

We treated the observed variability in near-hourly dolphin eDNA concentrations as a combination of variability in production and loss processes along with observational stochasticity (Figure 3). Fitted parameter values will be discussed here using the posterior median estimate (Table 1), and 95% upper and lower confidence intervals are (Table S2 in Supporting Information S1). The drop off from the first time step in all models was a model edge effect that comes from fitting μ_{init} (Figure 3), which had an uninformitive prior and wide confidence intervals in all models (Table S2 in Supporting Information S1).

The M4 Mixed-state dolphin model had the lowest WAIC, indicating that it had the best predictive accuracy relative to model complexity (Table 1). In M4, eDNA production alternated between $\beta = 1.34$ copies mL^{-1} dolphin^{-1} produced in the 70 min sampling period during the low-shedding state and $\beta(1 + \phi) = 127$

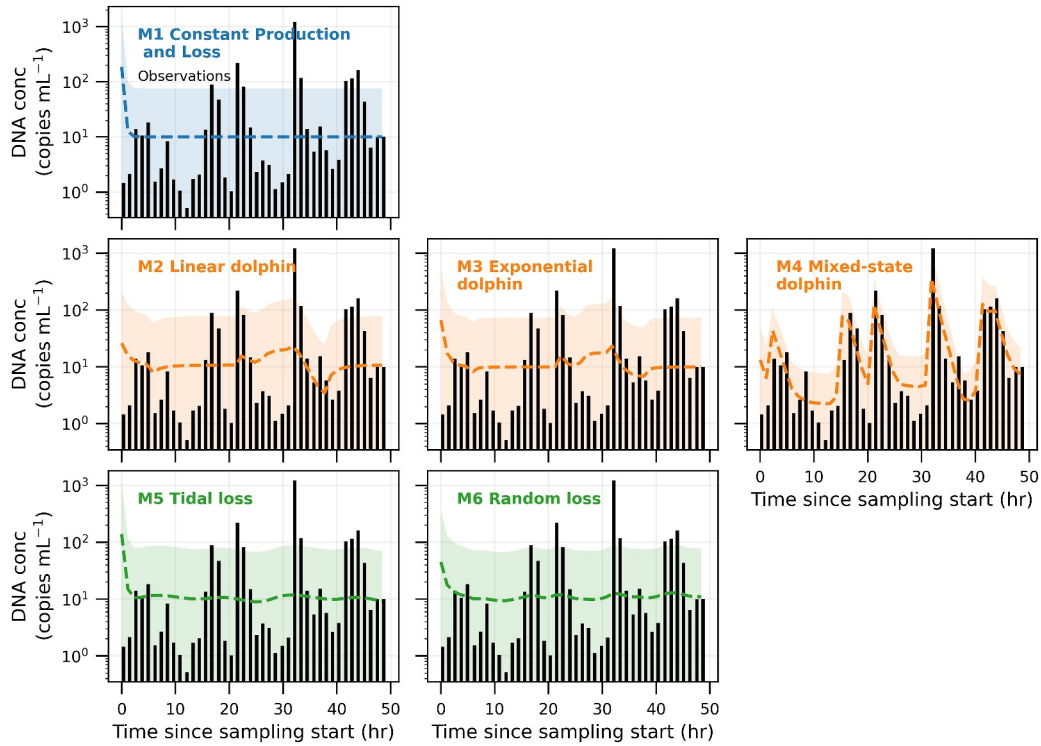

Figure 3. Comparison of process models (summarized in Table 1). Black bars are observed eDNA concentrations in copies mL^{-1} of filtered seawater. In each plot, dashed lines represent the posterior median of the model-predicted concentration of eDNA. Top row model in dashed blue has neither production nor loss variability. Middle row models in dashed orange test production variability. Bottom row models in dashed green test loss variability while having no production variability. Pale shading indicates observation variance expected around model predictions.

copies mL^{-1} dolphin^{-1} per sampling period during the high-shedding state (Table 1). Therefore, DNA production was about one hundred times greater in sampling periods characterized as elevated shedding states (see ϕ in Table 1). The probability rate that a sampling period would be in high-shedding state was $p = 0.16$ dolphin^{-1} (note probability of elevated shedding state scaled with N_t in Equation 3). The persistence fraction of eDNA was estimated as $\alpha = 0.33$, indicating 67% of eDNA was lost across each 70 min sampling period. Although M4 performed best, the CV of the observation model, $\theta = 1.41$, was greater than one and the credibility intervals were wide (transparent shading in Figure 3). For comparison, the CV of the biological replicates taken nearest to the pen during the transect sampling was 0.16. However, all other process models resulted in θ values at or greater than 2 (Table 1). Therefore, the features of the M4 Mixed-state dolphin model of eDNA production were able to capture the high variability seen in this dolphin eDNA time series that the variable eDNA loss or simpler eDNA production models could not.

The other process models performed less well. Observation variance alone (M1 Constant Production and Loss model) could not explain the time-variability in the data. Although eDNA shedding is often assumed to be linearly or exponentially related to animal abundance, neither the M2 Linear dolphin model nor M3 Exponential dolphin model performed well in this study. Time-variation in loss given constant shedding could not reproduce the dolphin eDNA trends either using tidal-variation (M5 Tidal loss) or unrestricted variation (M6 Random loss). Especially since M6 Random loss only performed marginally better than M1 Constant Production and Loss, the eDNA production flexibility in the M4 Mixed-state dolphin model remains the most likely explanation for the variability in the time series.

An hourly loss rate of 0.57 hr^{-1} was converted from the per-sampling-period loss rate in the M4 Mixed-state dolphin model by Equation 4. The 95% confidence interval on Loss range from 0.48 to 0.67 hr^{-1}.

3.2. Part 2: Calculating Contributions to eDNA Loss

In the water sampled by the ESP, the best fitting model suggested 57% of eDNA was lost each hour to degradation, advection, and diffusion. Below, we quantify the loss rates due to biological decay and physical transport and diffusion to determine their relative significance.

3.2.1. Biological Decay Experiment

The decay experiment examined the loss of dolphin eDNA concentrations due to biological degradation by isolating dolphin water from the environment. Dolphin eDNA concentration decreased from its initial value at an exponential decay rate of 0.020 hr^{-1} with a 95% confidence interval of 0.021–0.18 hr^{-1} (Figure S1 in Supporting Information S1). This is consistent with reported ranges for marine waters at 7° C (Lamb et al., 2022).

3.2.2. Physical Transport and Diffusion

The transect samples demonstrate an overall decrease in eDNA concentration with increasing distance from the source animals after being transported by ocean currents. As expected, being further from the animals, transect samples had eDNA concentrations far lower than those in the ESP samples adjacent to the netted enclosure. The highest estimated eDNA concentrations in transect samples among technical replicates was 2.74 copies mL^{-1}, which was from the sampling station located nearest to the dolphin enclosures. eDNA concentrations generally decreased with distance. The mean observed eDNA concentrations increased slightly from 100 to 300 m as well as the variability across the biological replicates. At the farthest sampling station (600 m away; northernmost blue circle in Figure 1b), all technical replicates quantified eDNA concentrations to be <0.1 copies μL^{-1} and in each biological replicate, one in three technical replicates did not amplify any dolphin eDNA. These data points were treated as zeroes when taking a mean. Using a linear regression of the log of the mean of technical and biological replicates at the sampling stations, we found eDNA concentrations decreased exponentially with distance at a rate of 0.01 copies $mL^{-1}m^{-1}$ (Figure 4a; blue line).

To convert this spatial loss rate to a temporal loss rate, we used the tracer model. The particle concentrations decreased with distance at a rate of 0.009 particles m^{-3} (Figure 4a; yellow line). Assuming particle concentrations m^{-3} distribute similarly to eDNA and form a probability density map, particle concentrations are expected to be proportional to eDNA concentrations in copies mL^{-1}. Model predictions were overall consistent with observations. A linear regression between the particle and mean eDNA concentrations at the sampling stations had a $R^2 = 0.99$, and a linear regression of the log of particle and eDNA concentrations had a $R^2 = 0.63$. Particle concentrations decreased in space and time at a rate the same order of magnitude as eDNA concentrations, although particle concentrations were proportionally higher at the farthest 600 m sampling location than the middle two sampling locations. The difference between the slopes in Figure 4a (indicating exponential spatial decrease rates) of particle and eDNA concentrations was only 10%, with observed eDNA decreasing slightly more rapidly.

Conversion from spatial to temporal loss rates was done using the average age of particles at the sampling location (Figure 4b). Mean age did not increase monotonically with distance because particles took nonlinear paths from release to their location at time of sampling. The mean particle age at the 600 m sampling location was younger than the 300 m sampling location. We used the age estimates from the particles at the sampling stations to convert spatial loss rate to temporal loss rate, acknowledging uncertainty in the particle statistics at the furthest sampling station. The decrease in particle concentration as a function of mean particle age was 0.45 hr^{-1}, which is our estimate for rate of eDNA loss due to environmental transport and diffusion (slope of orange line in Figure 4). The transport and diffusion loss rate estimate is an order of magnitude larger than the biological degradation rate of 0.02 hr^{-1} estimated in the laboratory decay experiment and much closer to the eDNA loss rate of 0.57 hr^{-1} estimated by the box model using the ESP time series in Part 1.

4. Discussion

Hourly variability in marine eDNA concentrations has been reported in field studies of fish metabarcoding (Jensen et al., 2022) and striped jack qPCR (Murakami et al., 2019) but without a mechanistic analysis of its causes. Here, we have used a set of observations from field, lab, and modeling studies to identify the likely roles of production, loss, and stochastic processes to explain variability of eDNA concentrations over space and time.

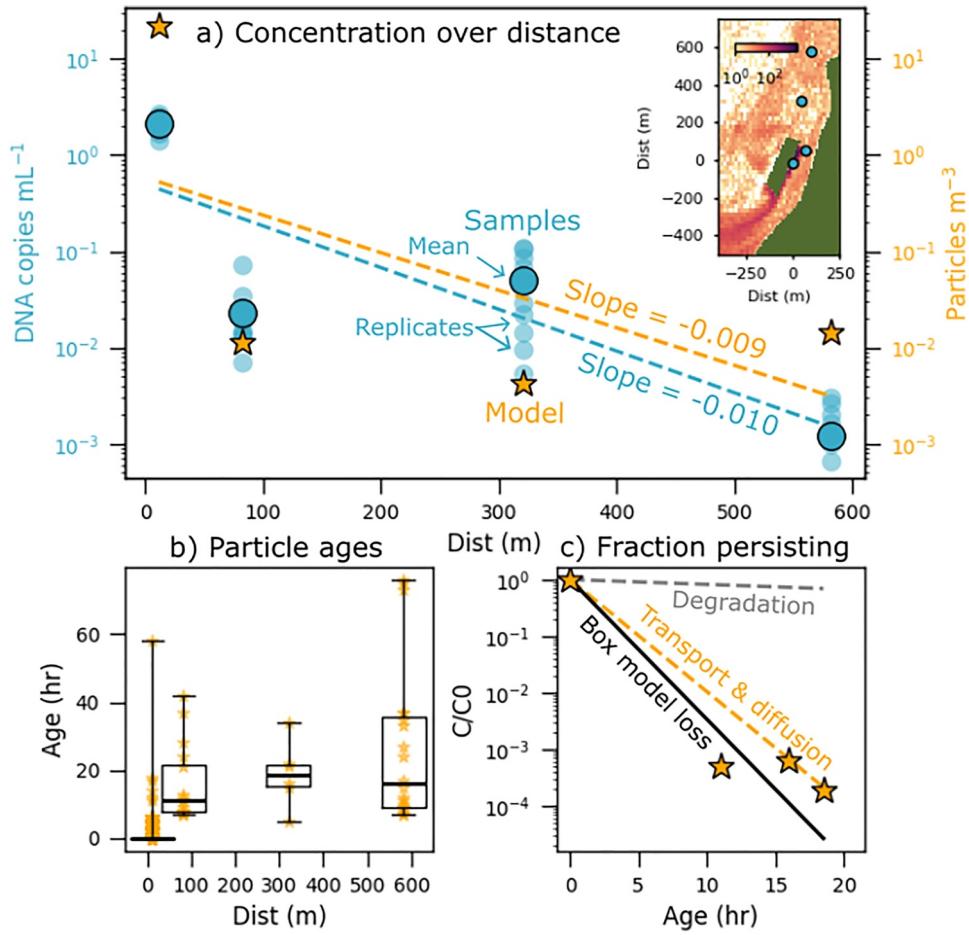

Figure 4. (a) Observed dolphin eDNA concentrations from transect sampling (blue circles, solid/outlined are means and transparent are individual replicates, left *y*-axis) compared with expected concentration of material distributed from netted dolphin enclosure by ocean processes using particles and a hydrodynamic model (orange stars, right *y*-axis) as a function of distance from netted dolphin enclosure. Modeled expectations were estimated using particle concentrations in upper 2 m and within 15 m radius of sampling locations from tracer model. Slopes of log-linear fits (dashed lines) demonstrate similarity in the magnitude of concentration loss across all sampling stations between observations and model. Inset shows map of sampling locations (blue circles) and surface particle distribution (heatmap) at time of sampling (3 February 2023 at 21:12:00 UTC). (b) Ages of particles at transect sampling location. Orange stars are individual particles, and box plots summarize particle age median (thick line) and quartiles. Box plot whiskers extend from minimum to maximum. (c) Decrease in eDNA concentration over time due to environmental transport and diffusion estimated from hydrodynamic model (orange stars and dashed line), biological degradation estimated from the decay experiment (gray dashed line), and all mechanisms estimated from the box model in Part 1 (black solid line).

Importantly, we find that (a) eDNA production varies over time and is well captured by the two-state model we employ here, (b) most—approximately 57%—of the target species' eDNA was lost each hour, (c) biological degradation explains only a small fraction of this loss, such that (d) oceanographic transport and diffusion likely explain most of the apparent eDNA loss in this marine system. Although the magnitudes of these processes will vary with the contextual details of any given eDNA study, this work establishes an important framework for understanding variability of eDNA concentrations over space and time more generally.

4.1. Primary Driver of Near-Hourly Variability in eDNA: Observation, Loss, or Production?

We wanted to explain the variability across these samples using a model with observation variability, loss variability, and production variability. The model evaluation criteria support eDNA production variability as the most likely explanation. Below, we discuss further evidence that observation stochasticity or loss variability could not account for the data peaks, and the possible nature of intermittent peaks in eDNA shedding.

Observation variability would be the primary driver of variability if eDNA production and loss were essentially constant but distributed heterogeneously through the sampling environment as in Yates et al. (2023). This could occur if the size distribution of particles bearing genetic material was skewed but consistent in time. Variance in particle size distribution of genetic material is not well understood. Cells may begin as clumps or form clumps over time through aggregation/flocculation (Yates et al., 2023). Environmental DNA clumps will break down into smaller pieces over timescales that have not been observed and are likely highly variable but are assumed to be on the order of a few hours based on fecal pellet literature (Allan et al., 2021). Thus, fresh eDNA clumps may appear to have lower mean abundance with higher variability than older, dis-aggregated genetic material (Brandão-Dias et al., 2023). The breakdown of genetic material into smaller and more homogeneously distributed particles over time is an alternative mechanical explanation to the eDNA-plume schematic proposed in some riverine eDNA literature (Augustine et al., 2024; Wood et al., 2021). However, the conceptual model with constant eDNA production and loss did not explain our data well. The sawtooth shape of the peaks suggests that abnormally high observations do not occur independently. Rather, samples with high eDNA concentrations co-occur with elevated concentrations in subsequent samples, more likely reflecting time-variation in ambient eDNA concentrations. Together with the low statistical support for models without variability in production or loss, observation variability can be ruled out as the primary driver of the temporal variability seen in these data.

Loss of eDNA between data points was significant in the process models of ESP data, but time-variability of loss rates is unlikely to explain the peaks in the time series. Loss variability could in theory be explained by slowed degradation of genetic material or reduced transport and flushing of the sampled water. However, the process model of loss variation with a tidal effect term had poor model performance, and tidal currents generally vary smoothly which would not produce the peak pattern seen in the ESP time series. This difference in the importance of tidal transport in the two sampling campaigns was very likely because the ESP was sheltered from currents by the concrete pier, illustrating the importance of oceanographic context in interpreting eDNA results. Losses via eDNA degradation could also vary, as degradation rate is known to change with temperature (Allan et al., 2020; McCartin et al., 2022). However, temperature changes are unlikely to explain eDNA peaks because temperature varies smoothly following a day/night cycle by a range around 5°C. Over that temperature range, decay rates in literature may change by up to a factor of 2 (Allan et al., 2020) but not enough to account for the hundred-fold magnitude in observed eDNA seen in the peaks.

Production variability would be the primary driver of variability if eDNA concentration fluctuations were due to variation in dolphin abundance or variation in amount of eDNA shed per individual dolphin. Although eDNA concentration has been correlated with fish abundance in shedding studies (Jo & Yamanaka, 2022), eDNA concentration here could not be explained by reported dolphin number alone (even allowing for uncertainty in reported dolphin number) because of the large peaks in the data. Variation in eDNA shedding per individual has not been well studied, although intermittent increases in eDNA shedding during feeding and defecation was given as a potential explanation for why striped jack eDNA concentrations did not decrease monotonically with distance from animals by Murakami et al. (2019). A mixed-state model where a background level of shedding is punctuated by episodic large injections of eDNA is biologically sensible and capable of fitting the data. Dolphins were fed fish in the netted enclosure as part of husbandry and fish consumption has a diuretic effect in Atlantic bottlenose dolphins, increasing fecal and urinary output for 8–10 hr (Ridgway, 1972), and defecation rate is presumed to correlate with feeding events in cetaceans (Jaquet & Whitehead, 1999). The frequency and volume of feeding during this study was not reported, and time until defecation following feeding is not known and assumed highly variable. However, defecation remains a very plausible explanation for eDNA peaks. An additional possible explanation is elevated skin cell sloughing. Bottlenose dolphins have high rates of skin cell sloughing in order to maintain a hydrodynamically smooth surface equivalent to replacing their outermost epidermal layer every 2 hours (Hicks et al., 1985). Elevated sloughing of skin cells likely occurs as dolphins interact physically with one another and their surroundings. Defecation remains the strongest explanation for the eDNA production peaks, but further investigation is warranted to determine the nature of large eDNA injections to better understand whether they will persist coherently downstream of the source.

4.2. eDNA Loss: Biological Degradation or Physical Transport and Diffusion?

By comparing the loss rates estimated in Part 1 with biological decay and transport and diffusion rates from the tracer model, we conclude that losses in the high-frequency dolphin eDNA time series are primarily due to physical processes. In locations where transport and diffusion are less important, such as in lakes (Yates et al., 2023) or bays

(Murakami et al., 2019), degradation may become relatively more important. Biological degradation may also be more important for warmer temperatures and different target species. Allan et al. (2020) found biological decay coefficients over $0.1 hr^{-1}$ for grass shrimp and moon jelly at around 20° C, which is large enough that degradation could be the leading order loss term in low-flow environments. For most marine and coastal applications, accurate estimation of transport and diffusion will be necessary for predicting eDNA abundance.

5. Conclusions

Environmental DNA is a powerful tool for monitoring and detecting occupancy for target species, but quantitative mechanistic frameworks for understanding observed eDNA abundances are hard to develop and validate. With a unique sampling opportunity around a managed population of non-native dolphins and a hydrodynamic ocean model, we were able to parse variability in eDNA production and biological and physical losses in Atlantic bottlenose dolphin eDNA concentration. Dolphin eDNA concentrations were highly variable across 70-min measurements. This variability may be a general result, but it will be especially true for marine mammals and other rare targets. The high frequency dolphin eDNA concentration time series was not linearly proportional to the reported number of dolphins in a netted enclosure next to the sampling site. Rather, the high frequency eDNA time series was characterized by sawtooth-shaped peaks, which suggest that eDNA production occurs as a mixed-state model which has background levels and episodic large eDNA injections. Every peak occurred at a time step when at least one dolphin was reported to be occupying the netted enclosure nearby the instrument. Further study is warranted on nature of these peaks in eDNA production to determine whether they result from biological processes that are generalizable to other species (like defecation) and whether peaks continue to characterize eDNA time series downstream. From fitting a loss rate in the high frequency time series, we found that, on average, 57% of eDNA was lost each hour. In comparing a biological degradation study against a tracer model of physical transport and diffusion, we determined that biological loss alone is insufficient to account for observed loss, and physical processes account for most of the loss. Although exact production and loss rates will be site specific and vary in time, these findings emphasize the importance of understanding eDNA production and loss mechanisms for quantitatively predicting and interpreting eDNA concentrations.

Data Availability Statement

The ESP, dolphin occupancy, and tide data and R NIMBLE model codes used for Part 1 are archived and available at https://zenodo.org/doi/10.5281/zenodo.12735445.

Acknowledgments
This material is based on research supported by the Office of Naval Research under Award Number (N00014-22-1-2719) Office of Naval Research, US Navy Pacific Fleet. We acknowledge that the land our laboratories are located on has been the home of Coast Salish people since time immemorial and that our study area encompasses the traditional and ancestral waters of the Coast Salish peoples and the Coastal Treaty Tribes of Washington. We thank Kevan Yamahara of the Monterey Bay Aquarium Research Institute for his assistance and advice configuring the ESP for deployment. We also thank Andrew Shelton and Len Thomas for their insightful conversations and technical assistance with statistical modeling. This study was supported through collaborative research efforts with the U.S. Navy's Marine Mammal Program. The authors are grateful to U.S. Naval Base Kitsap-Bangor for logistic support.

References

Allan, E. A., DiBenedetto, M. H., Lavery, A. C., Govindarajan, A. F., & Zhang, W. G. (2021). Modeling characterization of the vertical and temporal variability of environmental dna in the mesopelagic ocean. *Scientific Reports*, *11*(1), 21273. https://doi.org/10.1038/s41598-021-00288-5

Allan, E. A., Kelly, R. P., D'Agnese, E. R., Garber-Yonts, M. N., Shaffer, M. R., Gold, Z. J., & Shelton, A. O. (2023). Quantifying impacts of an environmental intervention using environmental dna. *Ecological Applications*, *33*(8), 1–21. https://doi.org/10.1002/eap.2914

Allan, E. A., Zhang, W. G., Lavery, A. C., & Govindarajan, A. F. (2020). Environmental dna shedding and decay rates from diverse animal forms and thermal regimes. *Environmental DNA*, *3*(2), 492–514. https://doi.org/10.1002/edn3.141

Augustine, B. C., Hutchins, P. R., Jones, D. N., Williams, J. R., Leinonen, E., & Sepulveda, A. J. (2024). A hierarchical model for edna fate and transport dynamics accommodating low concentration samples. *bioRxiv preprint*, 1–61. https://doi.org/10.1101/2024.03.27.586987

Baetscher, D. S., Pochardt, M. R., Barry, P. D., & Larson, W. A. (2024). Tide impacts the dispersion of edna from nearshore net pens in a dynamic high-latitude marine environment. *Environmental DNA*, *6*(2), 1–11. https://doi.org/10.1002/edn3.533

Brandão-Dias, P. F. P., Hallack, D. M. C., Snyder, E. D., Tank, J. L., Bolster, D., Volponi, S., et al. (2023). Particle size influences decay rates of environmental dna in aquatic systems. *Molecular Ecology Resources*, *23*(4), 756–770. https://doi.org/10.1111/1755-0998.13751

Carraro, L., Mächler, E., Wüthrich, R., & Altermatt, F. (2020). Environmental dna allows upscaling spatial patterns of biodiversity in freshwater ecosystems. *Nature Communications*, *11*(3585), 1–12. https://doi.org/10.1038/s41467-020-17337-8

Cerco, C. F., Schultz, M. T., Noel, M. R., Skahill, B., & Kim, S. (2018). A fate and transport model for asian carp environmental dna in the chicago area waterways system. *Journal of Great Lakes Research*, *44*(4), 813–823. https://doi.org/10.1016/j.jglr.2018.04.010

Collins, R. A., Wangensteen, O. S., O'Gorman, E. J., Mariani, S., Sims, D. W., & Genner, M. J. (2018). Persistence of environmental dna in marine systems. *Nature Communications Biology*, *1*(8), 1–11. https://doi.org/10.1038/s42003-018-0192-6

de Valpine, P., Paciorek, C., Turek, D., Michaud, N., Anderson-Bergman, C., Obermeyer, F., et al. (2024a). NIMBLE: MCMC, particle filtering, and programmable hierarchical modeling. [Computer software manual]. https://doi.org/10.5281/zenodo.1211190

de Valpine, P., Paciorek, C., Turek, D., Michaud, N., Anderson-Bergman, C., Obermeyer, F., et al. (2024b). NIMBLE user manual. [Computer software manual]. https://doi.org/10.5281/zenodo.1211190

de Valpine, P., Turek, D., Paciorek, C., Anderson-Bergman, C., Temple Lang, D., & Bodik, R. (2017). Programming with models: Writing statistical algorithms for general model structures with NIMBLE. *Journal of Computational & Graphical Statistics*, *26*(2), 403–413. https://doi.org/10.1080/10618600.2016.1172487

Ely, T., Barber, P. H., Man, L., & Gold, Z. (2021). Short-lived detection of an introduced vertebrate edna signal in a nearshore rocky reef environment. *PLoS One*, *16*(6), e0245314. https://doi.org/10.1371/journal.pone.0245314

Fukaya, K., Murakami, H., Yoon, S., Minami, K., Osada, Y., Yamamoto, S., et al. (2020). Estimating fish population abundance by integrating quantitative data on environmental dna and hydrodynamic modelling. *Molecular Ecology*, *30*(13), 3057–3067. https://doi.org/10.1111/mec.15530

Gelman, A., & Rubin, D. B. (1992). Inference from iterative simulation using multiple sequences. *Statistical Science*, *7*(4), 457–472. https://doi.org/10.2307/2246093

Goldberg, C. S., Turner, C. R., Deiner, K., Klymus, K. E., Thomsen, P. F., Murphy, M. A., et al. (2016). Critical considerations for the application of environmental dna methods to detect aquatic species. *Methods in Ecology and Evolution*, *7*(11), 1299–1307. https://doi.org/10.1111/2041-210X.12595

Hicks, B. D., St. Aubin, D. J., Geraci, J., & Brown, W. (1985). Epidermal growth in the bottlenose dolphin, *Tursiops truncatus*. *Journal of Investigative Dermatology*, *1*, 60–63.

Jaquet, N., & Whitehead, H. (1999). Movements, distribution and feeding success of sperm whales in the pacific ocean, over scales of days and tens of kilometers. *Environmental DNA*, *25*, 1–13.

Jensen, M. R., Sigsgaard, E. E., de Paula Ávila, M., Agersnap, S., Brenner-Larsen, W., Sengupta, M. E., et al. (2022). Short-term temporal variation of coastal marine edna. *Environmental DNA*, *4*, 747–762. https://doi.org/10.1002/edn3.285

Jo, T., Arimoto, M., Murakami, H., Masuda, R., & Minamoto, T. (2019). Estimating shedding and decay rates of environmental nuclear dna with relation to water temperature and biomass. *Environmental DNA*, *2*, 140–151. https://doi.org/10.1002/edn3.51

Jo, T., & Yamanaka, H. (2022). Fine-tuning the performance of abundance estimation based on environmental dna (edna) focusing on edna particle size and marker length. *Ecoloy and Evolution*, *12*(8), e9234. https://doi.org/10.1002/ece3.9234

Keller, A. G., Grason, E. W., McDonald, P. S., Ramón-Laca, A., & Kelly, R. P. (2022). Tracking an invasion front with environmental dna. *Ecological Applications*, *32*(4), 1–18. https://doi.org/10.1002/eap.2561

Kutti, T., Johnsen, I. A., Skaar, K. S., Ray, J. L., Husa, V., & Dahlgren, T. G. (2020). Quantification of edna to map the distribution of cold-water coral reefs. *Frontiers in Marine Science*, *7*(446), 1–12. https://doi.org/10.3389/fmars.2020.00446

Lamb, P. D., Fonseca, V. G., Maxwell, D. L., & Nnanatu, C. C. (2022). Systematic review and meta-analysis: Water type and temperature affect environmental dna decay. *Molecular Ecology Resources*, *22*(7), 2494–2505. https://doi.org/10.1111/1755-0998.13627

Lutscher, F., Pachepsky, E., & Lewis, M. A. (2005). The effect of dispersal patterns on stream populations. *Society for Industrial and Applied Mathematics*, *47*(4), 749–772. https://doi.org/10.1137/050636152

MacCready, P., McCabe, R. M., Siedlecki, S. A., Lorenz, M., Giddings, S. N., Bos, J., et al. (2021). Estuarine circulation, mixing, and residence times in the salish sea. *Journal of Geophysical Research: Oceans*, *126*(2), e2020JC016738. https://doi.org/10.1029/2020JC016738

Mass, C. F., Albright, M., Ovens, D., Steed, R., Maciver, M., Grimit, E., et al. (2003). Regional environmental prediction over the pacific northwest. *Bulletin of the American Meteorological Society*, *84*(10), 1353–1366. https://doi.org/10.1175/BAMS-84-10-1353

McCartin, L. J., Vohsen, S. A., Ambrose, S. W., Layden, M., McFadden, C. S., Cordes, E. E., et al. (2022). Temperature controls edna persistence across physicochemicalconditions in seawater. *Environmental Science and Technology*, *56*(12), 8629–8639. https://doi.org/10.1021/acs.est.2c01672

Metzger, E. J., Smedstad, O. M., Thoppil, P. G., Hurlburt, H. E., Cummings, J. A., Wallcraft, A. J., et al. (2014). Us navy operational global ocean and arctic ice prediction systems. *Oceanography*, *27*(3), 32–43. https://doi.org/10.5670/oceanog.2014.66

Mofjeld, H. O., & Larsen, L. H. (1984). Tides and tidal currents of the inland waters of western Washington (Vol. ERL PMEL-56; NOAA Technical Memorandum). *Pacific Marine Environmental Laboratory*.

Murakami, H., Yoon, S., Kasai, A., Minamoto, T., Yamamoto, S., Sakata, M. K., et al. (2019). Dispersion and degradation of environmental dna from caged fish in a marine environment. *Fisheries Science*, *85*(2), 327–337. https://doi.org/10.1007/s12562-018-1282-6

Ramón-Laca, A., Wells, A., & Park, L. (2021). A workflow for the relative quantification of multiple fish species from oceanic water samples using environmental dna (edna) to support large-scale fishery surveys. *PLoS One*, *16*(9), e0257773. https://doi.org/10.1371/journal.pone.0257773

Ridgway, S. H. (1972). Homeostasis in the aquatic environment. In S. H. Ridgway (Ed.), *Mammals of the sea: Biology and medicine* (pp. 590–747). Charles C Thomas.

Scholin, C. A., Birch, J., Jensen, S., Marin, R., Massion, E., Pargett, D., et al. (2018). The quest to develop ecogenomic sensors: A 25-year history of the environmental sample processor (esp) as a case study. *Oceanography*, *30*(4), 100–113. https://doi.org/10.5670/oceanog.2017.427

Sepulveda, A. J., Birch, J. M., Barnhart, E. P., Merkes, C. M., Yamahara, K. M., Marin, R., et al. (2020). Robotic environmental dna bio-surveillance of freshwater health. *Scientific Reports*, *10*(14389), 1–8. https://doi.org/10.1038/s41598-020-71304-3

Shchepetkin, A. F., & McWilliams, J. C. (2005). The regional oceanic modeling system (roms): A split-explicit, free-surface, topography-following-coordinate oceanic model. *Ocean Modelling*, *9*(4), 347–404. https://doi.org/10.1016/j.ocemod.2004.08.002

Shea, D., Frazer, N., Wadhawan, K., Bateman, A., Li, S., Miller, K. M., et al. (2022). Environmental dna dispersal from atlantic salmon farms. *Canadian Journal of Fisheries and Aquatic Sciences*, *79*(9), 1377–1388. https://doi.org/10.1139/cjfas-2021-0216

Shogren, A. J., Tank, J. L., Andruszkiewicz, E. A., Olds, B., Mahon, A. R., Jerde, C. L., & Bolster, D. (2017). Controls on edna movement in streams: Transport, retention, and resuspension. *Scientific Reports*, *7*, 1–11. https://doi.org/10.1038/s41598-017-05223-1

Shogren, A. J., Tank, J. L., Egan, S. P., Bolster, D., & Riis, T. (2019). Riverine distribution of mussel environmental dna reflects a balance among density, transport, and removal processes. *Freshwater Biology*, *64*(8), 1467–1479. https://doi.org/10.1111/fwb.13319

Visser, A. (1997). Using random walk models to simulate the vertical distribution of particles in a turbulent water column. *Marine Ecology Progress Series*, *158*, 275–281. https://doi.org/10.3354/meps158275

Walz, K., Yamahara, K., Michisaki, R. P., & Chavez, F. P. (2019). Mbari environmental dna (edna) extraction using qiagen dneasy blood and tissue kit. *Moss Landing, CA*. [Computer software manual]. https://doi.org/10.17504/protocols.io.xjufknw

Watanabe, S. (2013). A widely applicable bayesian information criterion. *Journal of Machine Learning Research*, *14*, 867–897. Retrieved from https://www.jmlr.org/

Wood, Z. T., Lacourseière-Roussel, A., LeBlanc, F., Trudel, M., Kinnison, M. T., Garry McBrine, C., et al. (2021). Spatial heterogeneity of edna transport improves stream assessment of threatened salmon presence, abundance, and location. *Frontiers in Ecology and Evolution*, *9*(650717), 1–16. https://doi.org/10.3389/fevo.2021.650717

Xiong, J., & MacCready, P. (2024). Intercomparisons of five ocean particle tracking software packages. *Geoscientific Model Development*, *17*(8), 3341–3356. https://doi.org/10.5194/gmd-17-3341-2024

Xiong, J., MacCready, P., Brasseale, E. A., Allan, E. A., Ramón-Laca, A., Parsons, K., et al. (2025). Advective transport drives environmental dna dispersal in an estuary. *Environmental Science and Technology*.

Yamahara, K. M., Demir-Hilton, E., Preston, C. M., Marin, R., Pargett, D., Roman, B., et al. (2015). Simultaneous monitoring of faecal indicators and harmful algae using an in-situ autonomous sensor. *Letters in Applied Microbiology*, *61*(2), 130–138. https://doi.org/10.1111/lam.12432

Yamamoto, S., Minami, K., Fukaya, K., Takahashi, K., Sawada, H., Murakami, H., et al. (2016). Environmental dna as a 'snapshot' of fish distribution: A case study of Japanese jack mackarel in maizuru bay, sea of Japan. *PLoS One*, *11*(3), e0149786. https://doi.org/10.1371/journal.pone.0149786

Yates, M. C., Gaudet-Boulay, M., Garcia Machado, E., Côté, G., Gilbert, A., & Bernatchez, L. (2023). How much is enough? Examining the sampling effort necessary to estimate mean edna concentrations in lentic systems. *Environmental DNA*, *00*, 0–14. https://doi.org/10.1002/edn3.461